

Identification of air shower radio pulses for the GRAND online trigger

Sandra Le Coz^{a,*} for the GRAND collaboration

^aSorbonne Université, CNRS/IN2P3, Laboratoire de Physique Nucléaire et de Hautes Energies, LPNHE, 4 place Jussieu, F-75005 Paris, France

E-mail: lecozsandra@yahoo.com

The Grand Radio Array for Neutrino Detection (GRAND) is an envisioned observatory that aims to detect the radio emission from air showers induced by ultra-high-energy cosmic particles; in particular, by neutrinos. Because these are rare, GRAND requires a large detection area, necessitating the use of inexpensive radio-detection units that must trigger autonomously. Such a trigger must achieve a high rejection efficiency of the dominant transient radio background, while keeping a high detection efficiency for air shower radio pulses. Fortunately, air shower simulations and field data suggest that air shower radio pulses exhibit characteristic features whose exploitation would lead to a powerful background rejection. We present the results of a machine learning signal classification method that has been tested on simulations and data recorded by a GRAND prototype in the Gansu province of China. Considering time traces that pass a simple 3σ -transients pre-trigger, a neural network is able to keep 66% of the air showers pulses for a Signal to Noise Ratio (SNR) between 3 and 4, and more than 86% after a SNR of 4, while rejecting between 97% and 99% of the background traces. This trigger method will eventually be implemented to the next prototypes to be tested under field conditions.

38th International Cosmic Ray Conference (ICRC2023)
26 July - 3 August, 2023
Nagoya, Japan



*Speaker

1. Introduction

The Giant Radio Array for Neutrino Detection (GRAND) is an ambitious proposal to instrument a total area of 200 000 km² with 200 000 radio antennas in the next decade. These antennas, grouped in sub-arrays of 10 000 units typically, deployed at favorable locations around the world, will form an observatory for Ultra-High Energy cosmic particles –and primarily, neutrinos– with unprecedented detection sensitivity and angular resolution (of the order 0.1° [1]). See [2, 3] for more details on GRAND.

For gigantic radio arrays such as GRAND to succeed in detecting UHE neutrinos and cosmic rays, we will need to develop large-scale autonomous radio detectors that reach similar levels of detection and reconstruction performance as externally triggered radio detectors. An effort has been initiated within the GRAND collaboration through the NuTrig proposal to achieve this goal [4]. In the present work, we focus on the First Level Trigger (FLT), i.e. the treatment developed within NuTrig to identify radio pulses associated with Extensive Air Showers (EAS) at the level of each antenna alone.

In section 2, we introduce the principle of an advanced FLT algorithm. In section 3, we present the data that are used to train and evaluate a neural network-based FLT. We then detail the neural network itself in section 4, the training process in section 5, and the results in section 6.

2. Principles of the First Level Trigger

Past [5, 6] or present [7] experiments which have attempted autonomous radio-detection of EAS use a rather simple trigger logic to decide if a transient signal measured at the antenna level may be considered for recording. Very often, a basic signal-over-threshold condition is used, where the threshold is set at a few times the stationary noise level. Even if more elaborated conditions on pulse shape, duration, or repetition rate might have been considered in some experiments, we believe a more elaborated treatment of the available information could be performed. We note in particular that the good understanding of the processes leading to electromagnetic emission by EAS now allow a reliable simulation of the pulses associated with EAS. In addition, the electromagnetic environment is continuously monitored by the radio antennas. This precise knowledge of both (EAS) signal and background can surely be used to build an advanced FLT.

In NuTrig, we are focusing on a neural network-based FLT. This FLT is motivated by a first successful study based on the TREND experimental data [8]. Hundreds of EAS candidates were identified within the TREND experimental data through an offline analytical algorithm, with a ~80% confidence level [9]. The time traces associated with these EAS candidates, and the same amount of random TREND background traces (that were rejected by the same identification algorithm), were used to train a neural network. When applied to a billion of recorded TREND traces, the neural network achieved a background rejection efficiency of 82% at the antenna level, and of 98% at the array level (where space-time coincidences between antenna-level triggers were requested), while 90% of the EAS candidates were successfully identified. This encouraging result led us to apply a similar method to the FLT for GRAND. While TREND antennas were monopolar, GRAND antennas are equipped with 3 perpendicular arms. Because EAS radio signals exhibit very specific

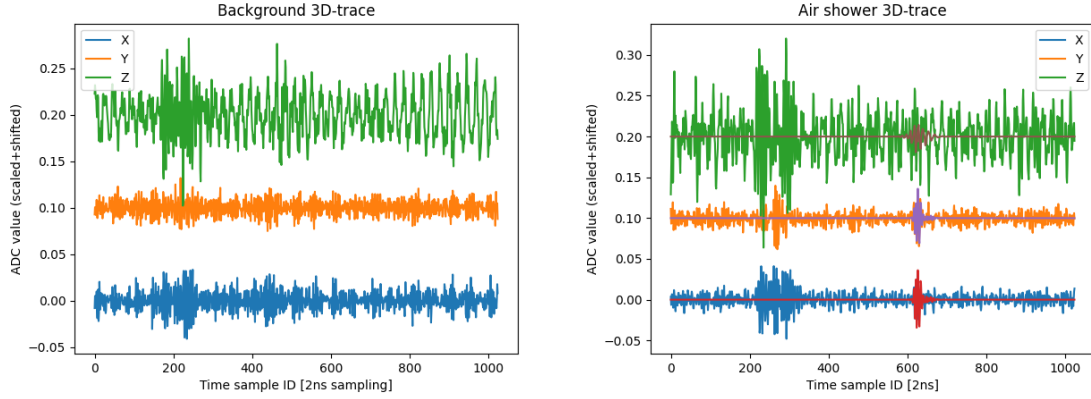


Figure 1: ‘Background’ (left) and ‘air shower’ (right) 3D-trace examples (blue, orange and green, for X, Y and Z channels, respectively). Traces are scaled (for training reasons) and vertically shifted (+0.1 for Y and +0.2 for Z, for illustration only). For the ‘air shower’ 3D-trace example (right), the air shower signal before the superimposition is shown in red, purple, and brown. This air shower signal belongs to the [4,5] SNR range, for the X and Y channels.

polarization features [10], that background pulses can hardly mimic, we were confident that better performances might be achieved for GRAND.

3. Datasets

The neural network datasets rely on the experimental data of GP13, a GRAND prototype composed of 13 butterfly antennas, deployed in a remote area of the Gobi desert, in the Gansu province of China [7]. During a running phase of 11 days in May 2023, 3-arms-traces of 2048 ns were recorded every 10 seconds.

The present study uses as an input a realistic reproduction of real run conditions. Prior to a neural network treatment, a simple yet efficient pre-trigger algorithm is applied : only traces with at least 2 points over 3σ within a time window of 25 ns are kept for further analysis. This treatment reject (useless) signals without detectable transients, and allows to restrict the finite neural network computation time for those of interest for the search of EAS. The following subsections describe the process to produce transients datasets, for a ‘background’ and a EAS (further referred as ‘air shower’) origin. When describing the process, ‘the maximum of the absolute value’ of a trace is simply referred as its ‘maximum’, to lighten the text.

3.1 Background datasets

Traces are randomly picked within 669 748 daytime GP13 experimental traces. They are selected if they pass the aforementioned windowed double 3σ pre-trigger, for at least 1 of the 3 channels, and if the maximum does not stand at the edges of the trace (see section 3.2.3). 10 000 ‘background’ 3D-traces, such as as the one on the left side of figure 1, are devoted to training, and another dataset of 10 000 3D-traces is dedicated to the test phase.

3.2 Air shower datasets

Because GP13 is still in a commissioning phase, no event could yet be tagged as a air shower radio candidate. Unlike the TREND neural network trigger study (see section 2), which only relied on experimental data, the present study ‘air shower datasets’ are thus semi-simulated. They are produced following several steps that are described below.

3.2.1 Air shower electric fields

In order to cover the full possible range of signal shapes, signal frequency spectra, and simulated signal over experimental noise ratio, that we would like to be able to trigger on, the air shower signal datasets must be generated from a various range of simulated air showers. We therefore use a simulation set containing air-shower-induced electric fields computed with ZHaireS [11], for an array of 277 antennas. The set covers the full azimuth range, zenith angles are between 30° and 87° , and core positions are within the array. The air showers come from protons and iron nuclei, of energies up to 4×10^{18} eV. We only selected air showers above 10^{18} eV, in order to obtain a significant portion of high signals.

3.2.2 Air shower ADC values

The simulated electric field is processed through the 3-arms butterfly GP13 antenna to obtain 3 open-circuit voltages. This simulated 3 open-circuit voltages are related to their respective antenna-arm effective length complex vector, which is simulated with NEC, as a function of the incoming electric field frequency. Each receiving antenna-arm acts as an independent voltage generator, for which the transmitted power depends on the matching between its own impedance and the impedance of its loaded remaining circuit.

Each of the 3 antenna-arms have its dedicated electronic route. After a balun, a matching network is included to obtain an improved impedance matching. It is connected to a 27 dB Low Noise Amplifier (LNA). Then, the air shower signal goes through a 3 m cable, connectors, a Variable Gain Amplifier (VGA) fixed at 20 dB, a 30-230 MHz pass-band frequency filter, and another balun, to finally be digitized through the Analog-to-Digital-Converter (ADC) at 500 Msps, for a length of 2048 ns (1024 samples), with a quantization of 2×2^{13} integer values for a $[-0.9V, +0.9V]$ ADC input range. All the electronic components have experimentally been characterized by a VNA (Vector Network Analyzer), which intend to provide their complex scattering-parameters as a function of the signal frequency. The combination of these parameters allows to get a valuable experimental calibration of the electronic response to the open-circuit antenna voltage.

The overall calibration (the antenna and its electronic) finally shows that, for a given projected electric field, the X and Y channels (horizontal arms) provide similar response, while Z (vertical arm) provides higher ADC values. This is consistent with the first GP13 experimental data (see figure 1, left).

3.2.3 Superimposition to background

The 3D-simulated air shower ADC signal is finally superimposed on a randomly picked experimental 3D-trace, to reproduce at best the process happening in reality. To avoid a bias due to the position of the air shower signal within this insertion trace, the simulated air shower signal is

randomly shifted. The shift must belong to the $[0,1848]$ ns range of the 2048 ns trace, not to cut part of the signal, which length is typically below 200 ns. To avoid a consequent bias, the ‘background’ and ‘air shower’ datasets have to satisfy a requirement on the position of the trace maximum. It must be at least 200 ns after the beginning of the trace, and at most 200 ns before its end. To be included in the ‘air shower’ datasets, the maximum of the air shower signal has to be at least 3 times the standard deviation of the experimental trace in which it is inserted, for at least one channel. We further refer to this as the ‘SNR’ requirement (Signal to Noise Ratio). After the superimposition, the trace has to pass the windowed double 3σ pre-trigger, as it is requested for the background datasets. The ‘air shower datasets’ finally consists in 3945 3D-traces that are devoted to training, and 6 SNR-ranges test-sets, for a total of 5266 traces, such as the one on the right side of figure 1.

4. Neural network

Neural networks are a powerful tool to find relationships between variables that are correlated at a high level of complexity, therefore hard to find with classical methods. Neural networks essentially consist in a succession of layers of variables, that are linearly combined (‘weighted’ and added) in different ways by neurons. The neurons are then activated with non-linear differentiable functions, to produce the next layer variables. A neural network is therefore theoretically able to approximate any function to fit the variables. The fit is performed (say the neural network is ‘trained’) by an algorithm that descends the gradient of a ‘loss’, that quantifies the fit error as a function of the fit-function weights. Instead of a classical fully connected neural network, where all the variables of a layer arise from their own set of weights, we used a CNN (Convolution Neural Network). CNN are devoted to find patterns by applying the same sets of weights (‘filters’), to a window sliding on the arranged variables. This weights-sharing between ranges of neurons makes the optimization process tremendously efficient for images recognition related tasks, such as our transient signals discrimination task.

In the present study, we use the Tensor Flow/Keras machine learning framework. The input variables of our neural network are the 3×1024 samples of our 3D 2048 ns traces. Because our task is a binary classification, the target outputs are 0 or 1, 1 being the label of the air shower class, 0 being the label of the background class. The output of the neural network would therefore be a number between 0 and 1, thus indicating the probability to belong to the air shower class. We chose to use 3 successive layers of convolution which kernel size is 11 (size of the sliding window), with 32 different filters per layer, with a ‘same’ padding (not to lose information at the end of the trace), and to activate the neurons with the ‘relu’ function. To focus on higher level features while reducing the computation load, we use a max-pooling layer of size 2 after each convolution layer. The network finally ends with a single-neuron layer, activated by a sigmoid, to confine the output values within the $[0,1]$ range.

5. Training

The training sets are represented on figure 2, by the distribution of the 3D-traces maximum, in standard deviation unit. Because inserting an air shower signal generally increases the standard deviation of the trace, the maximum of the trace in standard deviation unit would decrease if the air

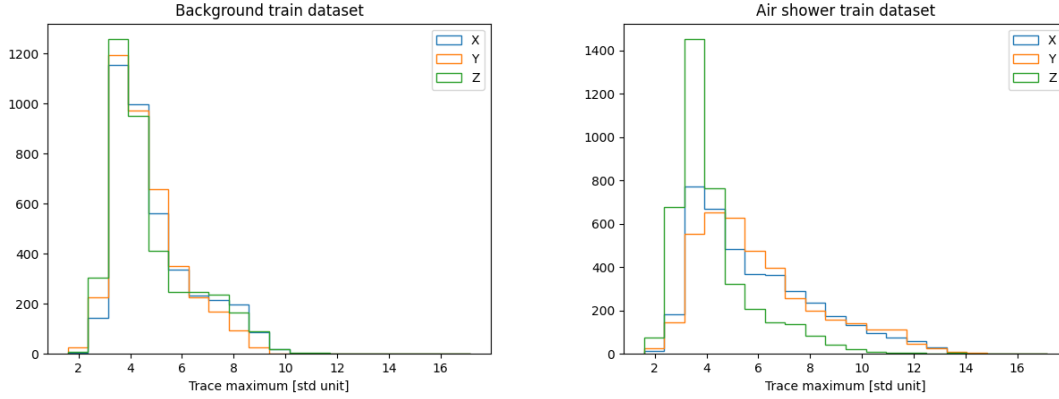


Figure 2: Distributions of the trace maximum, for the 3 channels, in respective standard deviation unit.

shower signal is not higher than the underlying background trace maximum. This is what generally happens for the Z channel (vertical arm), for which air shower electric fields are expected to be faint. Also as expected, the X and Y channels (horizontal arms) are on the contrary dominated by the air shower signal on a significant part of the set. At a future stage, we will study if this distinctive feature can be exploited by a (more classical) less resource-consuming discrimination method. However, trainings on 1D or 2D traces (not detailed in this document) show that, while the neural network performances decrease if we consider one channel only, they are not significantly affected by only getting rid of the Z channel.

The ‘background’ training set has been limited to 3945 instances, to match the size of the ‘air shower’ set, in order to perform a class-balanced training. The full dynamic range of the 3D-traces has been rescaled to $[-1,+1]$, for numerical reasons that ease the training. We chose to train our neural network with the ‘adam’ algorithm, for 80 epochs (one epoch is when all the training instances have been used once), with a batch size of 128 (number of instances that are used per weight-update iteration). Since the task is a classification, we chose the binary cross-entropy loss, which evolution is shown on the left side of figure 3. The performances are also evaluated for a validation set, which is a 10% subset of the training set, not used to descend the gradient. It allows to check all along the process that overfitting does not arise (orange curve on figure 3). Overfitting means the neural network is failing at extracting, from the training data, an underlying model that can fit unseen data as well. To avoid overfitting, we chose to use a dropout of 0.5 after each max-pooling layer. Additionally to the loss, the performances on the training set are also evaluated with a more comprehensible metric, the accuracy, which is the proportion of instances that are well classified. The right side of figure 3 shows that the accuracy has reached 95% at the end of the class-balanced training, for a decision threshold of 0.5.

6. Results

In this section, we evaluate the performances of the trained neural network on the test-dedicated sets. For air showers, data overlap between training and test sets has no chance to occur. For background, the overlap is estimated to be 2 instances or less, with a probability of 99%. Results

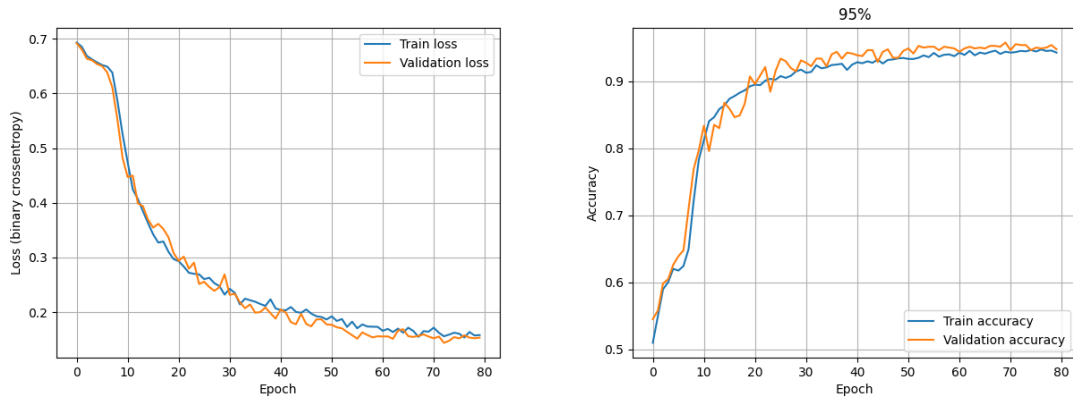


Figure 3: Loss and accuracy of the neural network as a function of the training epoch.

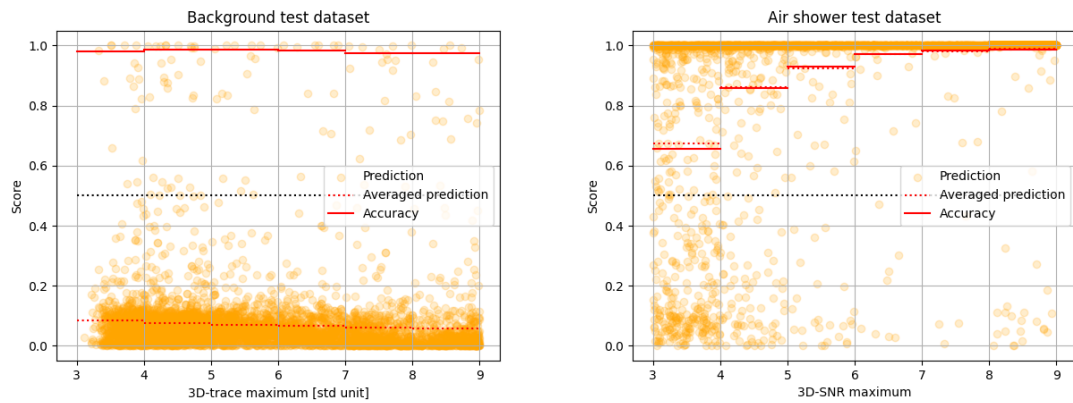


Figure 4: Performances of the neural network on the background and air shower test sets. The neural network predictions (the outputs), for all the input instances (the 3D-traces), are shown as orange dots. The dotted red lines are the respective bin-averaged predictions. The plain red lines are the respective bin-averaged accuracies for a 0.5 decision threshold. The [8,9] bin actually contains all the instances with SNR beyond 8. The dotted back line is the decision threshold.

are summarized in figure 4. For background (left), scores are arranged as a function of the input 3D-trace maximum in standard deviation unit, for 10 000 instances. For air showers (right), scores are shown for 6 sets of 3D-SNR floor maximum, from 3 to beyond 8, respectively containing [1050, 761, 532, 395, 314, 2214] instances. The floor SNR are randomly spread in their respective bin, for illustration only.

The accuracy is the proportion of orange dots that are below 0.5 for background, and above 0.5 for air showers. Considering this decision threshold of 0.5, the plain red lines show a background rejection rate between 97% and 99%, that does not significantly depend on the standard deviation related maximum. Regarding the air shower signals, one can note that, despite generally being outshined by transients in their background insertion trace, the ability to trigger on SNR between 3 and 4 has reached 66%. The accuracy then increases to 86% and more after a SNR of 4. The decision threshold can be adapted to trade off efficiency for purity, or conversely.

7. Conclusion

We have presented a preliminary neural network FLT study for GRAND. This study relied on the first GP13 data, and on air shower simulated signals. We showed that, after a 3σ -transients pre-trigger, a neural network can trigger on 66% of the air shower signals for a SNR between 3 and 4, and on more than 86% after a SNR of 4, while rejecting between 97% and 99% of the background traces. These performances need to be compared to what can be achieved by classical and less resource-consuming methods. This neural network promising trigger will be implemented on the GRAND acquisition board, to be first tested under laboratory controlled acquisition conditions. Once the trigger is validated, it will be tested on the field. The signals it will trigger on will be compared to air shower signals expectations, and to signals that classical algorithms trigger on. This would assess real conditions performances and allow to verify the neural network decision is not depending on simulation artifacts.

Acknowledgment

This work is supported by the ‘Emergences’ and ‘Initiative des 2 Infinis’ programs of Sorbonne Université, and by the Programme National des Hautes Energies of CNRS/INSU with INP and IN2P3, co-funded by CEA and CNES. It is a part of the NuTRIG project, supported by the ANR (ANR-21-CE31-0025) and the DFG (Projektnummer 490843803). Simulations were performed using the computing resources at the CCIN2P3 Computing Centre (Lyon/Villeurbanne – France), a partnership between CNRS/IN2P3 and CEA/DSM/Irfu.

References

- [1] V. Decoene *et al.* *PoS ICRC2021* (2021) 211.
- [2] GRAND Collaboration, J. Álvarez-Muñiz *et al.* *Sci. China Phys. Mech. Astron.* **63** no. 1, (2020) 219501.
- [3] GRAND Collaboration, J. Torres de Mello Neto *PoS ICRC2023* (these proceedings) 1050.
- [4] GRAND Collaboration, P. Correa *et al.* *PoS ICRC2023* (these proceedings) 990.
- [5] T. Asch, *Self-triggering of radio signals from cosmic ray air showers*. PhD thesis, Karlsruhe U., 2009.
- [6] D. Ardouin *et al.* *Astropart. Phys.* **34** (2011) 717–731.
- [7] GRAND Collaboration, P. Ma *et al.* *PoS ICRC2023* (these proceedings) 304.
- [8] S. Le Coz *et al.* *PoS ARENA2022* 041.
- [9] D. Charrier *et al.* *Astropart. Phys.* **110** (2019) 15–29.
- [10] S. Chiche *et al.* *Astropart. Phys.* **139** (2022) 102696.
- [11] J. Álvarez-Muñiz *et al.* *Phys. Rev. D* **86** (2012) 123007.